

金@银核壳纳米粒子的制备和形貌的精确控制 及其表面增强拉曼光谱性能

刘晓宇 张东杰 张慧娟 张丛筠* 刘亚青*
(中北大学功能纳米复合材料山西省重点实验室, 太原 030051)

摘要: 用种子生长法制备了金 @ 银核壳结构的纳米粒子。在制备过程中通过控制氯金酸的浓度和硝酸银的体积, 得到了不同粒径的金核和不同厚度的银壳构成的核壳纳米粒子。从而得到了具有不同 SERS 性能的金 @ 银核壳纳米粒子。选取具有最佳 SERS 性能的金 @ 银核壳纳米粒子实现了对罗丹明 6G 的微量检测。

关键词: 金 @ 银核壳纳米粒子; 表面增强拉曼光谱; 罗丹明 6G

中图分类号: O614.122; O614.123 文献标识码: A 文章编号: 1001-4861(2018)04-0712-07

DOI: 10.11862/CJIC.2018.012

Synthesis of Au@Ag Core-Shell Nanoparticles for Sensitive Surface-Enhanced Raman Scattering by Precisely Adjust Its Morphology

LIU Xiao-Yu ZHANG Dong-Jie ZHANG Hui-Juan ZHANG Cong-Yun* LIU Ya-Qing*
(Shanxi Province Key Laboratory of Functional Nanocomposites, School of Materials Science and Engineering, North University of China, Taiyuan 030051, China)

Abstract: Au@Ag core-shell nanoparticles were prepared by seed-mediated growth method. The plasmon resonance properties of the core-shell nanoparticles are highly dependent on the size and shape of the core and thickness of the shell, which could be simply adjusted by varying the concentration of HAuCl₄ and the volume of AgNO₃. The prepared core-shell nanoparticles exhibit excellent SERS performance as substrate to detect rhodamine 6G (R6G). In addition, the precise control of core-shell morphologies (core size and shape, the thickness of the shell) is of significant importance as it strongly determines the overall SERS performance in micro chemical detection.

Keywords: Au@Ag core-shell nanoparticles; SERS; rhodamine 6G

0 Introduction

Surface enhanced Raman spectroscopy (SERS) is a significant and useful analytical technique, which was widely used in environmental monitoring^[1-2], food security^[3-4], chemical analysis^[5-7] and health care^[8-9]. It can be applied for label-free detection and provides specific spectral fingerprint of target molecules which

could be up to single-molecule level^[10-12]. It is generally recognized that the conduction electrons of metal materials generate a fantastic resonant oscillation with light irradiation, leading to tremendous electromagnetic enhancement in the adjacent areas of metal surfaces^[11-13]. Currently, Au and Ag nanoparticles with different sizes and shapes have attracted considerable attention in SERS field due to their outstanding local

收稿日期: 2017-07-05。收修改稿日期: 2017-09-12。

山西省青年科学家自然科学基金(No.2015021078)项目资助。

*通信联系人。E-mail: lyq@nuc.edu.cn, z.congyun@nuc.edu.cn

surface plasmon resonance (LSPR) properties^[14-16]. Bimetallic hybrid nanomaterials with combination of multiple plasmon coupling have distinct advantages compared with single component nanoparticles. Many strategies have been developed to construct alloy^[17-19], core-shell^[20-25], dendrite *etc.*^[26-29]. In these systems, the combination of bimetallic hybrid nanomaterials could influence metallic electronic states, which further influence the SERS enhancement^[28,30].

Core-shell nanocomposites, representing a novel nanostructure with adjustable core size, and tunable shell thickness, have been widely researched and used because of its excellent optical property. Yang et al. reported the preparation of Ag@Au core-shell nanocubes by galvanic replacement-free deposition^[23]. In this case, the surface plasmonic properties of Ag@Au core-shell nanocubes show a 5.4-fold enhancement due to chemical enhancement. Patra et al. prepared Ag@Au core-shell nanoparticles as Single-molecule surface-enhanced Raman scattering substrate, wherein the limit detection can be down to femtomole level by employing bianalyte technique^[24]. Recently, Song et al. prepared Au@Ag core-shell nanoparticles by seed growth method as a highly sensitive and selective SERS substrate for the detection of As(III)^[25]. Its detection limit of this substrate for As(III) is $3.1 \times 10^{-7} \text{ mg} \cdot \text{L}^{-1}$. Au@Ag core shell composite nanoparticles have been demonstrated to exhibit significant SERS performance. However, it is still challenging to precisely control the morphology of the core-shell nanoparticle.

In this paper, a reliable method for the preparation of Au@Ag core-shell nanospheres is reported. The seed-mediated growth method is used to synthesize the Au core. With the presence of reduction agent L-Ascorbic Acid, the AgNO_3 is reduced to Ag atoms and then deposited on the Au surface to form the shell. In this progress, the surface plasmon properties and the SERS activities can be adjusted by controlling the size of the Au core and the thickness of the Ag shell. The controlling method is easily performed by changing the concentration of HAuCl_4 and the volume of AgNO_3 . Finally, the morphology and properties of

Au@Ag core-shell nanospheres are characterized by UV-Vis adsorption spectra, Transmission Electron Microscope (TEM) and Raman measurement. The Au@Ag core-shell nanospheres with best SERS performance is used as SERS substrates to detect rhodamine 6G at ultralow concentration, indicating its excellent SERS sensitivity.

1 Experiment

1.1 Materials

Chloroauric acid and silver nitrate were purchased from Alfa Aesar. Hexadecyl trimethyl ammonium bromide (CTAB), *N*-Hexadecyltrimethylammonium chloride (CTAC), Sodium borohydride and L-Ascorbic Acid (AA) were purchased from Shanghai Chinese medicine Reagent. Sodium hydroxide and ethanol were obtained from Tianjin North founder Reagent Factory. All of the chemical reagents were analytical grade and used without further purification. Ultra pure water (resistivity of $18.2 \text{ M}\Omega \cdot \text{cm}$) was used through all of the experiments.

1.2 Synthesis of Au@Ag core-shell nanospheres

The Au@Ag core-shell nanospheres were synthesized by two steps. Au cores were synthesized by a typical method with a little modification^[31]. Specifically, 0.32 g CTAB was introduced into 10 mL ultrapure water, followed by the introduction of 0.2 mL HAuCl_4 ($0.01 \text{ mol} \cdot \text{L}^{-1}$) under magnetic stirring in an water bath at 30°C . Subsequently, 0.5 mL NaBH_4 ($0.01 \text{ mol} \cdot \text{L}^{-1}$) was added. After stirring for 5 min, the solution was undisturbed for 3 h. Finally, the Au seeds (about 14 nm) were prepared, which were utilized to grow larger Au core. Then, CTAC (0.32 g) was dissolved into 10 mL HAuCl_4 aqueous solution, followed by the addition of 4 mL AA ($0.1 \text{ mol} \cdot \text{L}^{-1}$) under magnetic stirring at 30°C . After several minutes, 0.3 mL Au nucleus was added, and then kept under undisturbed for 4 hours. In this progress, the size and the shape of Au core can be simply controlled by changing the concentration of HAuCl_4 .

The second step is to synthesize Au@Ag core-shell nanospheres. Briefly, 0.3 mL of the suspended Au seeds and CTAC (10 mL, $0.1 \text{ mol} \cdot \text{L}^{-1}$) were

introduced into a glass vial, followed by the addition of 0.5 mL AA ($0.1 \text{ mol} \cdot \text{L}^{-1}$) under magnetic stirring. Subsequently, different volumes of AgNO_3 ($0.1 \text{ mol} \cdot \text{L}^{-1}$) were added into the solution. Then, 0.1 mL NaOH ($0.01 \text{ mol} \cdot \text{L}^{-1}$) was titrated into the mixture. After reaction for 2 h, the product was collected by centrifugation and washed by ultra pure water. In this progress, the thickness of Ag shell was controlled by changing the volume of AgNO_3 .

1.3 Characterization

In this experiment, optical characterization of samples was performed on UV/Vis-4802 Ultraviolet and visible spectrophotometer (Unico Company Limited). The morphology and structures of samples were characterized by transmission electron microscope (TEM, JEOL 2100F) operating at an accelerating voltage of 100 kV. High-resolution TEM (HRTEM) images were recorded at an acceleration voltage of 200 kV.

1.4 SERS measurements

The SERS performance of the nanoparticles was

tested by Renishaw Invia Raman spectrometer. The prepared Au@Ag core-shell nanoparticle aqueous suspensions were injected into R6G aqueous solutions with different concentrations (10^{-4} , 10^{-5} , 10^{-6} , 10^{-7} , 10^{-8} , $10^{-9} \text{ mol} \cdot \text{L}^{-1}$) and stirred for 10 min. The mixed solutions were dropped on Si wafer and dried in the air for SRES measurement. The acquisition time was 1 s, and 532 nm laser with 1.2 mW power was used as excitation source.

2 Results and discussion

2.1 Characterization of the Au seeds

In typical synthesis, the homogeneously dispersed Au nanoparticles with spherical morphology and average diameter of 14 nm are fabricated as seeds (Fig.1(a,b)). The UV-Vis absorption spectrum of brown Au seed aqueous suspensions (inset in Fig.1c) exhibits a surface plasmon resonance (SPR) band at 510 nm which is in accordance with the size of Au seeds.

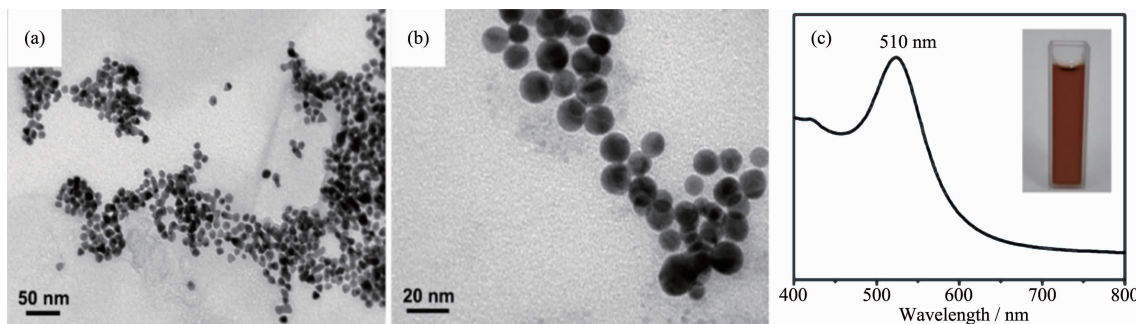


Fig.1 (a, b) TEM images with different magnification of Au seeds; (c) UV-Vis absorption spectra of Au seeds suspension and its digital image

2.2 Characterization of the prepared Au core

The SERS performance of metal substrate depends largely on the size and shapes of metal nanoparticles. In order to obtain an optimal morphology and the best SERS performance, a series Au cores with different size and shapes were prepared. Fig.2a shows that the color of Au core aqueous suspensions appears light red at first and gradually become dark red. Fig.2(b~f) show the SEM images of the Au cores prepared with different concentrations of HAuCl_4 ($c=0.1, 0.2, 0.3, 0.4$ and $0.5 \text{ mmol} \cdot \text{L}^{-1}$). At lower concentrations (0.1

and $0.2 \text{ mmol} \cdot \text{L}^{-1}$), many spherical nanoparticles with uniform size of 20 and 28 nm are formed, shown as the Fig.2(b,c). With the increasing dosage amount of HAuCl_4 aqueous solutions, the size of the Au cores increases gradually. At a higher concentration of $0.3 \text{ mmol} \cdot \text{L}^{-1}$, the nanoparticles aggregate and evolve into spheroidal nanoparticles with inhomogenous size distribution (Fig.2d). Upon increasing the concentration (0.4 and $0.5 \text{ mmol} \cdot \text{L}^{-1}$), more and more polyhedron structures appear with average diameter of 40 nm, such as octahedron, decanedron (Fig.2(e,f)). The

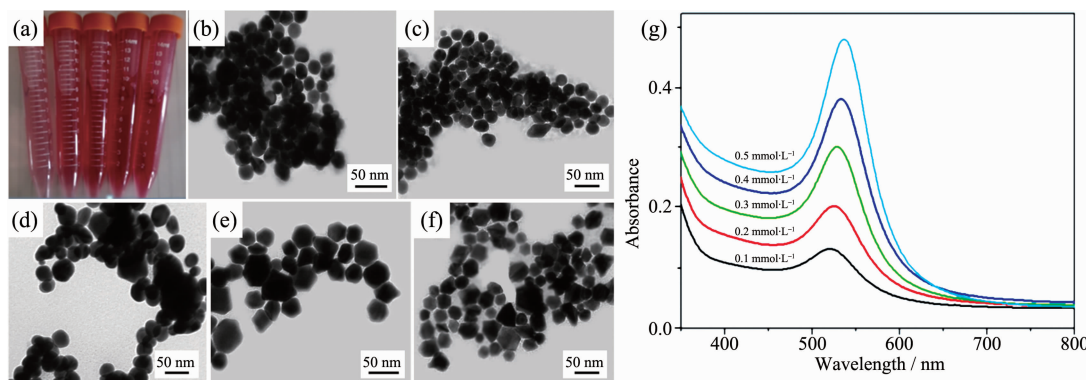


Fig.2 (a) Digital image of Au core aqueous suspensions; (b-f) TEM images of Au cores with different concentrations of HAuCl₄; (b) 0.1 mmol·L⁻¹, (c) 0.2 mmol·L⁻¹, (d) 0.3 mmol·L⁻¹, (e) 0.4 mmol·L⁻¹, (f) 0.5 mmol·L⁻¹; (g) UV-Vis absorption spectra of Au cores suspension with different concentrations of HAuCl₄

corresponding UV-Vis adsorption spectra (Fig.2g) show distinct SPR band of Au cores which progressively red-shift as the overall particle size increased. In addition, the intensity of SPR band of Au cores are increased, indicating that more Au cores were formed with the increasing dosage amount of HAuCl₄. The Au nanoparticles prepared from 0.2 mmol·L⁻¹ HAuCl₄ solutions are adopted as the cores for the fabrication of core-shell nanostructures.

2.3 Characterization of the Au@Ag core-shell nanoparticles

One of the significant advantages of core-shell nanoparticles is their adjustable plasmon resonance property. Apart from the tunable size of Au core, the thickness of Ag shell can be varied by changing the volume of AgNO₃. As shown in Fig.3(a-e), the average size of Au@Ag core-shell nanoparticles is varied from

30 to 38 nm depending upon the shell thickness, with the increasing amount of AgNO₃ solution, the color of the nanoparticle aqueous suspensions gradually becomes deeper (Fig.3f). The Au@Ag core-shell nanostructures are further identified by HR-TEM. As shown in Fig.4(a-e), it is distinguished that Ag shell with different thickness has been successfully wrapped around Au cores. When the volume of AgNO₃ solution is 50 μL, a very thin Ag shell with the thickness of about 2 nm is observed on the surface of Au core (Fig.4a). The shell thickness increases with increasing amount of AgNO₃. Fig.4b clearly shows that when the dosage amount of AgNO₃ solution was 75 μL, Ag shell with the average thickness of 4.5 nm was observed. While the dosage amount of AgNO₃ solution is varied from 100 to 125 μL, the shell thickness increases from 6.7 to 8.5 nm (Fig.4(c,d)).

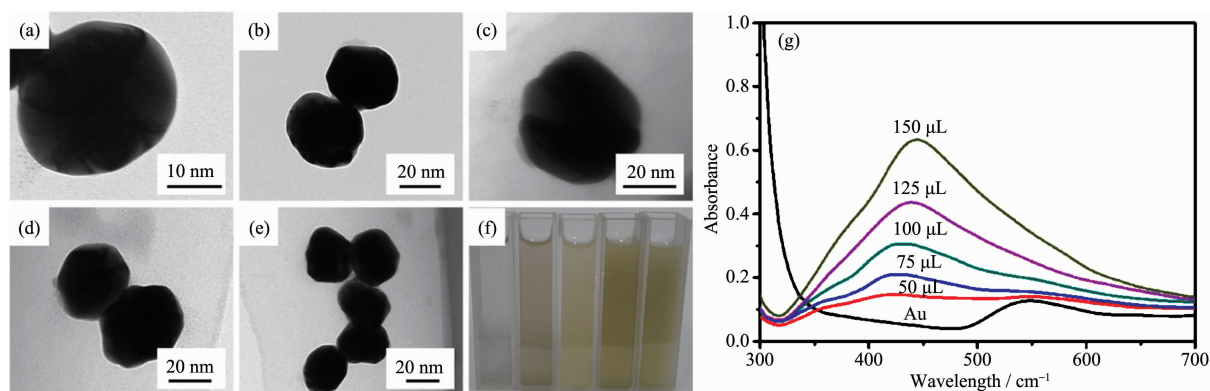


Fig.3 (a-e) TEM images of Au@Ag core-shell nanoparticles with different volumes of AgNO₃ solution: (a) 50 μL, (b) 75 μL, (c) 100 μL, (d) 125 μL, (e) 150 μL; (f) Digital image of Au@Ag core-shell nanoparticles aqueous suspensions prepared with different volumes of AgNO₃; (g) UV-Vis absorption spectra of Au@Ag core-shell nanoparticles suspension with different volumes of AgNO₃

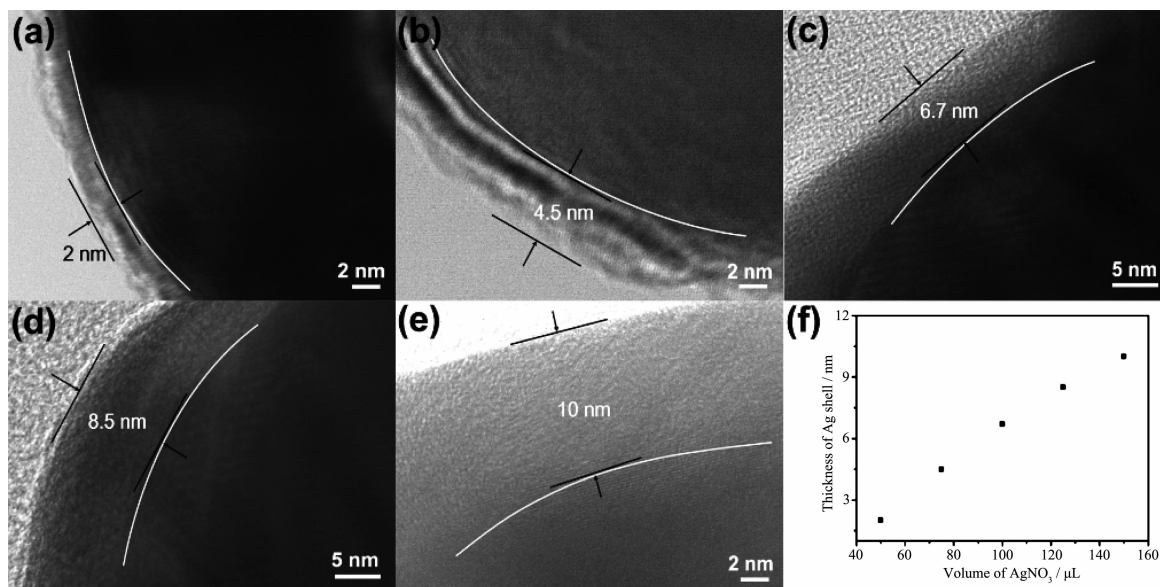


Fig.4 (a~e) HR-TEM images of Au@Ag core-shell nanoparticles with different volumes of AgNO₃ solution: (a) 50 μL, (b) 75 μL, (c) 100 μL, (d) 125 μL, (e) 150 μL; (f) Relationship between the thickness of Ag shell and the volume of AgNO₃ solution

Further increase in dosage amount of AgNO₃ solution (150 μL), the Ag shell reaches 10 nm in thickness (Fig.4e). As a result, the thickness of Ag shell shows a linear dependence on the volume of AgNO₃ solution (Fig.4f). It is probably that higher dosage amount of Ag precursor allows for the gradual deposition of Ag atoms on the surface of Au core, leading to form thicker shell. The corresponding UV-Vis adsorption spectra (Fig.3g) show distinct SPR properties of Au@Ag core-shell nanoparticles. With the increasing dosage amount of AgNO₃ solutions, a new band is gradually emerged around 430 nm and the intensity increases as more Ag is reduced, along with a significant red shift which due to the dielectric properties of silver. In addition, the SPR band at 525 nm which belong to Au is gradually disappeared because of the Ag shell.

2.4 SERS performance

To investigate the SERS performance, all of these Au@Ag core-shell nanoparticles are used as SERS substrates to detect R6G. Fig.5 shows the Raman spectra of R6G molecules (10^{-6} mol·L⁻¹) adsorbed on the Au@Ag core-shell nanoparticle substrate synthesized with different volumes of AgNO₃ solutions. Typical Raman spectra of R6G with clear peaks at 613, 776, 1 185, 1 312, 1 360, 1 364, 1 511, 1 576

and 1 651 cm⁻¹ are observed. Obviously, there are remarkable differences in SERS ability, the Au@Ag core-shell nanoparticles with diameter of 36.5 nm and thickness of 8.5 nm exhibit the highest SERS performance. Thus, it can be concluded that the Au core and Ag shell can produce the best bimetallic synergistic effect and further generate excellent SERS activities.

To further investigate the SERS ability of the Au@Ag core-shell nanoparticles, as shown in Fig.6a,

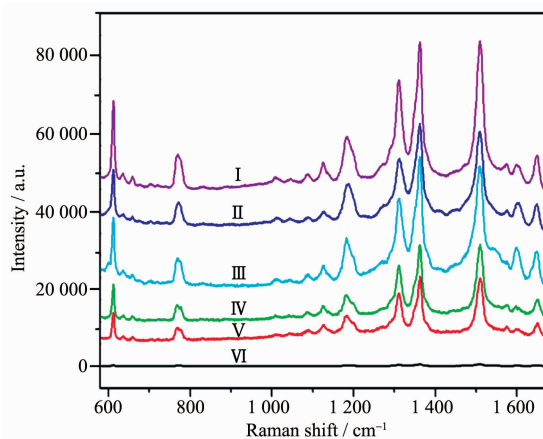


Fig.5 SERS spectra of R6G with different SERS substrates; Substrate prepared with different volume of AgNO₃ solution: (I) 125 μL, (II) 100 μL, (III) 150 μL, (IV) 75 μL, (V) 50 μL and (VI) without any substrates

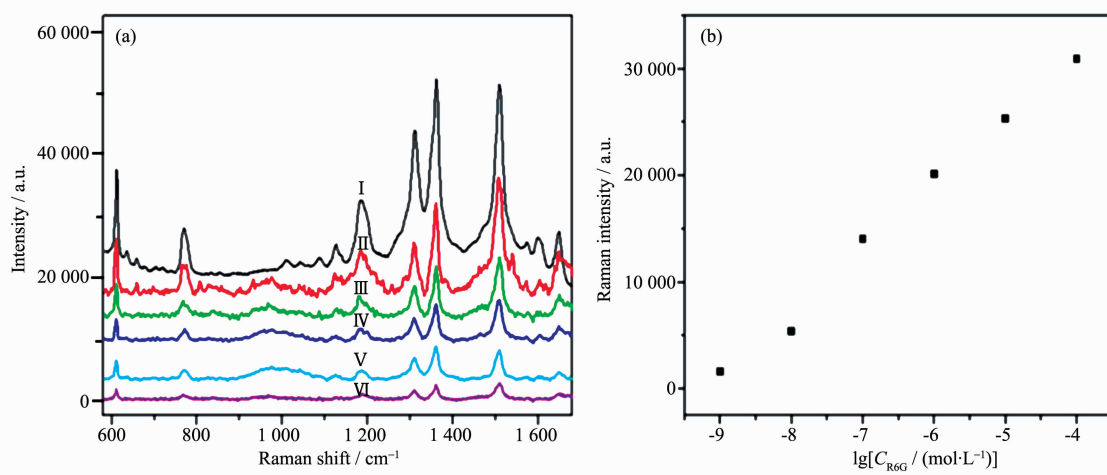


Fig.6 (a) SERS spectra of R6G with different concentration: (I) 10^{-4} mol·L⁻¹, (II) 10^{-5} mol·L⁻¹, (III) 10^{-6} mol·L⁻¹, (IV) 10^{-7} mol·L⁻¹, (V) 10^{-8} mol·L⁻¹, (VI) 10^{-9} mol·L⁻¹; (b) Linear fit calibration curve of the R6G molecules with concentrations from 10^{-9} to 10^{-4} mol·L⁻¹ on the Au@Ag core-shell nanoparticles

Raman spectra of R6G solution with different concentrations were detected by using the Au@Ag core-shell nanoparticles (the volume of AgNO₃ solution is 125 μL) as substrates. The intensity of SERS signal decreases according to the concentration of R6G decreases. However, it can still be recognized even the concentration of R6G is down to 10^{-9} mol·L⁻¹. The detection limit is extremely low compared to the bare Au or Ag nanoparticles in the current literature. This indicates that the detection limit for R6G is 10^{-9} mol·L⁻¹ in this system. To demonstrate the capability of the quantitative detection of R6G, the linear curves are showed in Fig.6b. The intensity of 1 364 cm⁻¹ peak has a good linear fit calibration curve.

Due to the outstanding SERS performance, Au@Ag core-shell nanoparticles are further investigated for detection of tetramethylthiuram disulfide, which is one of the most widely used insecticide. As shown in Fig.7, different concentrations of tetramethylthiuram disulfide were detected by using the Au@Ag core-shell nanoparticles (the volume of AgNO₃ solution is 125 μL) as substrates. The detection limit of tetramethylthiuram disulfide is 10^{-8} mol·L⁻¹, which is lower than the maximal allowed limit of 2.9×10^{-8} mol·L⁻¹ set by the U.S. Environmental Protection Agency (EPA). Such detection sensitivity suggesting that these Au@Ag core-shell nanoparticles are capable of an ultrasensitive chemical detection and have broad

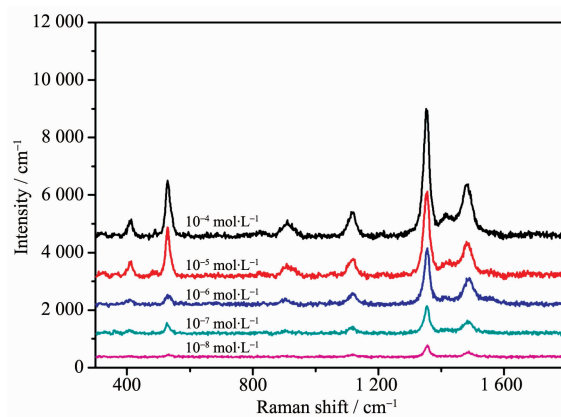


Fig.7 SERS spectra of tetramethylthiuram disulfide with different concentration

applications in various fields.

3 Conclusions

In conclusion, the Au@Ag core-shell nanoparticles with high SERS activity have been successfully synthesized. The Au core size/shape and the Ag shell thickness can be simply adjusted by varying the concentrations of HAuCl₄ and the volumes of AgNO₃ solution, respectively. The Au@Ag core-shell nanoparticles with different morphologies exhibit distinct SERS properties. The optimized Au@Ag core-shell nanoparticles, which were prepared with $0.2 \text{ mmol} \cdot \text{L}^{-1}$ HAuCl₄ and 125 μL AgNO₃, corresponding to 28 nm diameter of Au core and 8.5 thickness of Ag shell. In addition, the prepared Au@Ag core-shell nanoparticles can be used as an effective platform for SERS

detection of R6G and tetramethylthiuram disulfide. The detection limit is 10^{-9} and 10^{-8} mol·L⁻¹, respectively, indicating that the Au@Ag core-shell nanoparticles can be used for ultrasensitive chemical detection in various fields like food Safety.

Acknowledgments: This work was supported by the Natural Science Foundation for Young Scientists of Shanxi Province of China (No.2015021078) and International Cooperation of Science and Technology Project in Shanxi Province of China (No.2014081006-2).

References:

- [1] Hidi I J, Heidler J, Weber K, et al. *Anal. Bioanal. Chem.*, **2016**,**408**:8393-8401
- [2] Yang L, Qin X, Jiang X, et al. *Phys. Chem. Chem. Phys.*, **2015**,**17**:17809-17815
- [3] Fang W, Zhang X, Chen Y, et al. *Anal. Chem.*, **2015**,**87**: 9217-9224
- [4] Gao M, Fang W, Ren J, et al. *Analyst*, **2016**,**141**:5195-5201
- [5] Zheng H, Ni D, Yu Z, et al. *Food Chem.*, **2017**,**217**:511-516
- [6] Ge J, Li Y, Wang J, et al. *J. Alloys Compd.*, **2016**,**663**:166-171
- [7] ZHOU Xin(周鑫), YAO Ai-Hua(姚爱华), ZHOU Tian(周田), et al. *Chinese J. Inorg. Chem.*(无机化学学报), **2014**,**30**(3): 543-549
- [8] Chen Y, Zhang Y, Pan F, et al. *ACS Nano.*, **2016**,**10**:8169-8179
- [9] Tian F, Conde J, Bao C, et al. *Biomaterials*, **2016**,**106**:87-97
- [10] Cao Q, Liu X, Yuan K, et al. *Appl. Catal. B*, **2017**,**20**:607-616
- [11] Tian Y, Wu P, Liu Q, et al. *Talanta*, **2016**,**161**:151-156
- [12] Chen K, Shen Z, Luo J, et al. *Appl. Surf. Sci.*, **2015**,**351**: 466-473
- [13] Reymond-Larunaz S, Saviot L, Potin V, et al. *Appl. Surf. Sci.*, **2016**,**389**:17-24
- [14] MAN Shi-Qing(满石清), XIAO Gui-Na(肖桂娜). *Chinese J. Inorg. Chem.*(无机化学学报), **2009**,**25**(7):1279-1283
- [15] Farkhari N, Abbasian S, Moshaii A, et al. *Colloids Surf. B*, **2016**,**148**:657-664
- [16] Anantharaj S, Sakthikumar K, Elangovan A, et al. *J. Colloid Interface Sci.*, **2016**,**483**:360-373
- [17] Li T, Vongehr S, Tang S, et al. *Sci. Rep.*, **2016**,**6**:37092
- [18] Yan Y, Radu A I, Rao W, et al. *Chem. Mater.*, **2016**,**28**: 7673-7682
- [19] Li S S, Song P, Wang A J, et al. *J. Colloid Interface Sci.*, **2016**,**482**:73-80
- [20] Runowski M, Goderski S, Paczesny J, et al. *J. Phys. Chem. C*, **2016**,**120**:23788-23798
- [21] Jin X, Mao A, Ding M, et al. *Appl. Spectrosc.*, **2016**,**70**: 1692-1699
- [22] Qiu L, Wang W Q, Zhang A W, et al. *ACS Appl. Mater. Interfaces*, **2016**,**8**:24394-24403
- [23] Yang Y, Liu J, Fu Z W, et al. *J. Am. Chem. Soc.*, **2014**,**136**: 8153-8156
- [24] Patra P P, Kumar G V P. *J. Phys. Chem. C*, **2013**,**4**:1167-1171
- [25] Song L, Mao K, Zhou X, et al. *Talanta*, **2016**,**146**:285-290
- [26] Li D, Liu J, Wang H, et al. *Chem. Commun.*, **2016**,**52**: 10968-10971
- [27] Chang K, Chung H. *RSC Adv.*, **2016**,**6**:75943-75950
- [28] Ji J, Li P, Sang S, et al. *AIP Adv.*, **2014**,**4**:031329
- [29] Huan T N, Kim S, Van T P, et al. *RSC Adv.*, **2014**,**4**:3929-3933
- [30] He R, Wang Y C, Wang X, et al. *Nat. Commun.*, **2014**,**5**: 4327
- [31] Zheng Y, Zhong X, Li Z, et al. *Part. Part. Syst. Char.*, **2014**, **31**:266-273